





Electron transport properties of molecular junctions with anharmonic double-well potentialsDexian Sun , Wenjing Zhao, Qiyuan Dai , Feifei Qiu, Liang Ma , and Guangjun Tian ^{*}*State Key Laboratory of Metastable Materials Science & Technology
and Key Laboratory for Microstructural Material Physics of Hebei Province,
School of Science, Yanshan University, Qinhuangdao 066004, People's Republic of China*

(Received 25 June 2021; revised 29 November 2021; accepted 1 December 2021; published 10 December 2021)

In the present paper, we investigated the electron transport properties of molecular junctions with anharmonic vibrations described by double-well potentials in the sequential tunneling regime. It was found that the suppression of the low-bias current caused by strong electron-vibration couplings under harmonic approximation, i.e., the Franck-Condon blockade effect, could be lifted in the case of symmetric double-well potentials. The removal of the Franck-Condon blockade effect is a result of the distribution of the ground vibrational wave function in the two wells. Such a feature also enables the Franck-Condon blockade effect to be restored by breaking the symmetry of the double-well potential. We further demonstrated that the special vibrational transition properties of asymmetric double-well potentials could enable the effective modulation of the charge transport properties of such molecular junctions in the Franck-Condon blockade region by inducing population in excited vibrational levels with external fields such as infrared excitation.

DOI: [10.1103/PhysRevB.104.245411](https://doi.org/10.1103/PhysRevB.104.245411)**I. INTRODUCTION**

Electron transport properties of molecular junctions have been extensively studied since the pioneering theoretical design of a molecular rectifier by Aviram and Ratner [1], which has led to significant development in the field of molecular electronics [2–8]. In typical molecular junctions, a molecule, with size at the nanometer scale, is trapped between metallic electrodes to serve as the conduction/function unit in the electric circuit. The charge transport properties of such tiny circuits are related to many factors including the molecule-electrode coupling condition, molecular conformation, electronic distributions of the molecule in the junction, etc., which have been shown to lead to rich functionalities [5–7,9–13].

The electron-vibration coupling effect, which arises from the interaction between the electronic and nuclear degrees of freedom, could also have strong influence on the charge transport properties of molecular junctions [4,14,15]. Such an effect is especially prominent in the weak molecule-electrode coupling limit where the electron transport process is dominated by incoherent sequential tunneling [15–18]. In the sequential tunneling regime, the tunneling electron could stay on the molecule for sufficiently long time periods and, consequently, lead to the charging or discharging of the molecule [4,15]. As a result, the electron transport process will lead to vibrational transitions that are determined by the electron-vibration couplings following the Franck-Condon (FC) principle [15,16,19]. Previously, the influence of the electron-vibration coupling effect on the charge transport properties of weakly coupled molecular junctions was system-

atically studied based on the displaced harmonic oscillators approximation [16–18,20]. Interesting transport phenomena such as FC blockade (FCB), which describes the low-bias current suppression effect, has been theoretically predicted [16] and experimentally verified [19,21,22]. The FCB effect is caused by strong electron-vibration couplings which is proportional to the displacement between the potential energy surfaces (PESs) of the two charging states involved in the transport process [19]. If such displacement is much larger than the zero-point motion of the molecule, it will cause the overlap between the corresponding vibrational wave functions of the low-lying vibrational transitions to be negligible. As a result, the transition rates for the low-energy vibrational transitions and, consequently, the low-bias currents, will be strongly suppressed, which then lead to the FCB effect.

Calculations beyond the harmonic approximation have also been performed previously with the aim of examining the anharmonic effect on the transport properties [23–27]. Notably, most of these studies are based on Morse or Morse-like potentials, which are quite reasonable because such potentials are more close to the realistic situations in molecules. In the present paper, we perform theoretical calculations on the charge transport properties of molecular junctions with vibrational potentials described by double well (DW) potentials. Such types of potentials are commonly associated with intramolecular rotational vibrations and can also be found in molecules with Jahn-Teller effect [28]. We show that the special structure of a symmetric DW potential could significantly reduce the FCB effect expected in harmonic cases under similar electron-vibration coupling strengths. Further calculations show that the FCB effect can be restored by breaking the symmetry of the two wells. Moreover, we demonstrate that the unique vibrational transition properties of the asymmetric DW potentials could be applied as an effective way in the

^{*}tian@ysu.edu.cn

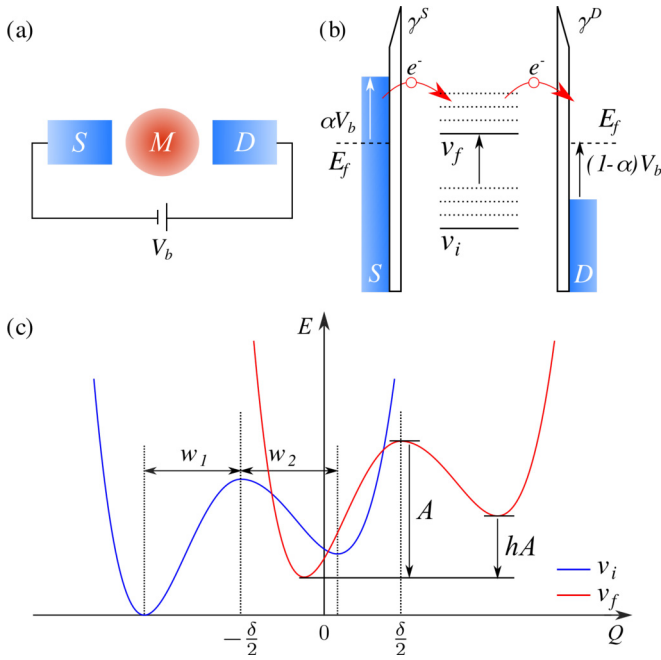


FIG. 1. (a) A schematic model of the molecular junction considered in the present paper. (b) Schematic diagram indicating the electron transport process of the molecular junction in the sequential tunneling regime. The bias coupling constant α has been set to 0.5. Symmetric molecule-electrode coupling strengths with $\gamma^S = \gamma^D = 1.0 \mu\text{eV}$ has been considered in the calculations. (c) The displaced double-well potentials that are used to describe the electron-vibration couplings. The initial state $|v_i\rangle$ (blue) and the final state $|v_f\rangle$ (red) are centered at $-\delta/2$ and $\delta/2$, respectively. The four dotted vertical lines are at the position where the potential slope is equal to 0.

modulation of the charge transport properties of the junction by applying appropriate external excitations such as infrared pumping in the FCB regime.

The rest of the paper is organized as follows. The theoretical model for the molecular junction in the sequential tunneling regime and the calculation method for the charge transport properties are given in detail in Sec. II. In Sec. III, we give the calculation results for molecular junctions described by both symmetric and asymmetric DW potentials and make direct comparisons to the more commonly studied harmonic potentials (HPs). In this section, we also investigate the possibility to modulate the charge transport property of molecular junctions described by asymmetric DW potentials by introducing external excitations that could lead to significant population in the excited vibrational energy levels. A summary of results is given in Sec. IV.

II. THEORETICAL MODEL AND CALCULATION METHOD

A. Theoretical model

A schematic representation of the molecular junction and the corresponding electron transport process are shown in Figs. 1(a) and 1(b), respectively. We assume that the molecule was weakly coupled to the source (S) and drain (D) electrodes with sufficiently small molecule-electrode coupling strengths

γ^S and γ^D . The electron transport process is dominated by sequential tunneling for such junctions. By applying a bias voltage (V_b), a potential window can be opened between the two electrodes, which can then initiate the transport process. In the following calculations, we have kept the bias coupling constant α to be 0.5, which leads to a symmetric bias drop on both electrodes.

As shown in Fig. 1(b), only two charging states v_i (initial state) and v_f (final state) were considered, which is based on the assumption that only one spin-degenerate energy level (can only be occupied by 0 or 1 electron) is involved in the transport process [17,29]. For the sake of simplicity, we have also assumed that the conducting level is aligned with the Fermi energy (E_f) of the electrodes at $V_b = 0$ V. This ensures the emergence of an electric current flow as soon as a nonzero bias voltage is applied.

B. Rate equation method

In the sequential tunneling regime, the charge transport properties of a molecular junction can be described by the rate equation method [16,17,27,29]. The time evolution of the occupation probabilities of the molecule in different levels (\mathbf{P} , which satisfies $\sum_m P_m = 1$) can be written in the matrix form as

$$\frac{d\mathbf{P}}{dt} = (\mathbf{R} + \mathbf{\Gamma})\mathbf{P}, \quad (1)$$

with \mathbf{R} and $\mathbf{\Gamma}$ being the tunneling rate matrix and a matrix describing vibrational decays within a given electronic state, respectively.

The off-diagonal elements of the tunneling rate matrix R_{mn} , with m and n belonging to different electronic states, describe the transition rates between vibrational energy levels and can be obtained from Fermi's golden rule [17,30]. If we assume the two electronic states involved in the transport process as the initial ($|v_i\rangle$) and final ($|v_f\rangle$) states with the latter containing one more electron, the tunneling rates between a pair of vibrational energy levels m and n belonging, respectively, to $|v_i\rangle$ and $|v_f\rangle$ can be written as [27]

$$\begin{aligned} R_{mn} &= F_{nm} \frac{\gamma^S}{\hbar} f(\epsilon^S) + F_{nm} \frac{\gamma^D}{\hbar} f(\epsilon^D), \\ R_{nm} &= F_{mn} \frac{\gamma^S}{\hbar} (1 - f(\epsilon^S)) + F_{mn} \frac{\gamma^D}{\hbar} (1 - f(\epsilon^D)), \end{aligned} \quad (2)$$

where

$$\begin{aligned} \epsilon^S &= \Delta\epsilon - \alpha eV_b, \quad \epsilon^D = \Delta\epsilon - (\alpha - 1)eV_b, \\ f(\epsilon) &= 1/(1 + e^{\epsilon/k_B T}). \end{aligned} \quad (3)$$

Here $f(\epsilon)$ is the Fermi function of the metallic electrodes, $\Delta\epsilon = \epsilon_{f,n} - \epsilon_{i,m}$ represents the energy difference between the two vibrational energy levels. F_{mn} and F_{nm} are the FC factors which are defined as the square of the overlap integral between the involved vibrational wave functions for the corresponding vibrational transitions. All of the other off-diagonal elements of \mathbf{R} are zero. The diagonal elements of \mathbf{R} can be obtained as

$$R_{kk} = - \sum_{k' \neq k}^{k'=1, N} R_{k'k}. \quad (4)$$

The relaxation matrix Γ in Eq. (1) describes the intraelectronic-state vibrational decays. In principle, the form of vibrational relaxations can be derived from first principles, where the relaxation time would be defined by the inverse of the diagonal element of the corresponding dissipation rates. The dissipation rates are defined by the strength of the system-bath coupling and bath spectral properties. For the sake of simplicity, in the present paper we assume that the molecule was coupled to a thermal bath consisting of a whole set of simple reservoir modes and adopt an *ad hoc* ansatz to describe the relaxation processes. In this form, only the off-diagonal matrix elements corresponding to intrastate relaxations and the diagonal elements will be nonzero. Consider m and n being two vibrational energy levels in the same electronic state; the nonzero elements of Γ can be calculated as [16,17,27,31]

$$\Gamma_{mn} = \frac{1}{\tau} \left(\frac{e^{-\epsilon_m/k_B T}}{\sum_{k'} e^{-\epsilon_{k'}/k_B T}} - \delta_{mn} \right), \quad (5)$$

where τ is the vibrational relaxation time, and δ_{mn} represents the Kronecker delta. In the simulations, τ has been set to 1 ns, which gives vibrational relaxations faster than the tunneling rate between the molecule and the electrodes ($\sim 2.4 \times 10^8 \text{ s}^{-1}$ for the considered coupling strength of 1 μeV). With such fast relaxations, the molecule will relax almost instantaneously to the thermal equilibrium during the electron transport process. For such equilibrium transport, the charge transport process is not expected to be significantly affected by the form of the vibrational relaxations. It is worthwhile to point out that, if the vibrational relaxation rates are close to or slower than the tunneling rates, the form in which the relaxations was incorporated could have significant influence on the charge transport process.

By solving the rate equations, the current of the molecular junction can be calculated by summing up the current flow through one of the electrodes as [17,27]

$$I = e \sum_{m \in i} \sum_{n \in f} (P_m R_{nm}^S - P_n R_{mn}^S). \quad (6)$$

Here R^S represents the contribution of the S electrode to the tunneling rates.

C. Vibrational potentials

In this paper, we mainly focus on the transport properties of molecular junctions with electron-vibration couplings described by displaced DW potentials. Figure 1(c) illustrates two displaced DW PESs in such a model. We assume that the two DW potentials have the same shape and differ with each other only by a displacement of δ . The magnitude of the displacement can be considered as a measure of the electron-vibration coupling strength, similar to the cases of HPs. We also introduced two parameters w_1 and w_2 to describe the width of each well in the DW potential. h is a parameter describing the height difference between the two wells. The inclusion of such parameters enables us to adjust the symmetry of the DW.

In this paper, three types of DW potentials, symmetric DW potential (SDWP), asymmetric DW potential with different well widths (ASDWP_w), and asymmetric DW potential with different heights (ASDWP_h) have been investigated. The PES

of the DW potential was defined as [32,33]

$$V(x) = \begin{cases} \frac{A[(x-x_0)^2 - w_1^2]^2}{w_1^4}, & x < x_0 \\ \frac{A(1-h)[(x-x_0)^2 - w_2^2]^2 + Ahw_2^4}{w_2^4}, & x \geq x_0, \end{cases} \quad (7)$$

with x_0 ($x_0 = \pm\delta/2$ for the two potentials) and A being the position and height of the energy barrier between the two wells. In the numerical simulations, A and w_1 have been set to 0.0046 a.u. (125 meV) and 50 a.u., respectively. These parameters were chosen in such a way that we can obtain a pair of characteristic near-degenerate vibrational energy levels below the energy barrier. Our test calculations for junctions with displaced SDWPs that support more than one pair of near-degenerate energy levels (achieved by increasing the barrier height A) indicates that the general features for the transport processes are very similar to those obtained with the applied parameters (details can be found in the Supplemental Material (SM) [34]). It should be mentioned that when electronic orbital degeneracies are involved, the singular coupling limit instead of the conventional weak-coupling limit has to be applied [35]. In the present paper, we considered only a single electronic orbital in the electron transport process and the energy (near) degeneracies are only associated with vibrational levels in the anharmonic potentials where the rate-equation method could still be applied [24]. It is also worthwhile to mention that pronounced high order tunneling processes such as cotunneling-assisted sequential tunneling [36] that are not included in the method used in the present paper could become important, especially at the strong electron-vibration coupling limit. However, as discussed by Leijnse and Wegewijs [36], such higher order processes are closely associated with the nonequilibrium vibrational distribution in the junction and the higher order features are not expected to play a significant role when the vibrational dissipation is fast, which is the case in our calculations. The other parameters were kept adjustable to exam the corresponding influence on the charge transport properties. As a comparison, the commonly studied model of displaced HPs were also included in the calculations. The two HPs were defined as

$$V_h(x) = \frac{\sqrt{A}}{w_1^2} (x - x_0)^2. \quad (8)$$

The four types of potentials together with the corresponding wave functions for the first five vibrational energy levels are shown in Fig. 2. Figure 2(a) shows the usual harmonic case with evenly spaced energy levels. For the SDWP ($w_1 = w_2 = 50$ a.u., $h = 0$ a.u.), as shown in Fig. 2(b), the most important change is that the first two vibrational levels (0 and 1) are near degenerate with both levels evenly distributed in the two wells [32,33]. Moreover, the energy spacing between vibrational energy levels is no longer a constant as for the HP. Figures 2(c) and 2(d) illustrate the vibrational energy levels for the two types of asymmetric DW potentials [33,37,38]. It can be found that breaking the symmetry of the two wells either by changing the width or height of one well can break the degeneracy of the first two vibrational levels. Moreover, the wave functions of these two levels are now each located in one of the wells instead of the even distributions as in the case of SDWP.

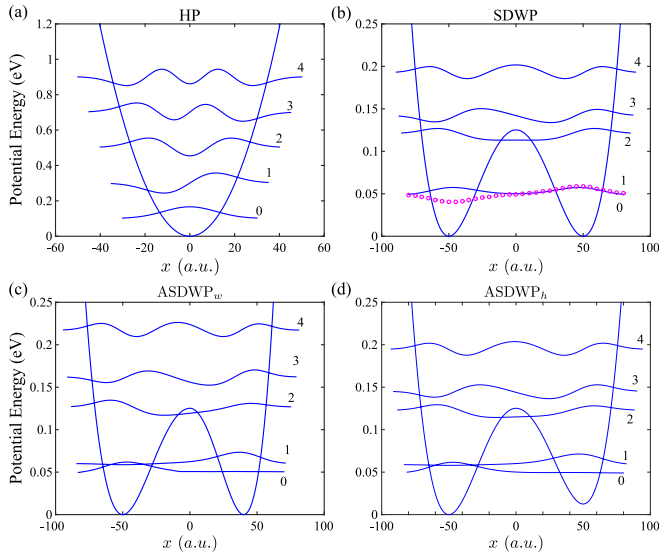


FIG. 2. Wave functions and corresponding vibrational energy levels of (a) harmonic potential, (b) symmetric double-well potential, in which the mauve circle lines represents the second vibrational energy level for the sake of distinction, (c) asymmetric double well potential with $w_2 = 0.80w_1$, $h = 0$, and (d) asymmetric double-well potential with $w_1 = w_2$, $h = 0.10$.

With the energy levels and corresponding wave functions in hand, the FC factors for the vibrational transitions of the displaced PES model can be conveniently obtained, which thus enables the calculations of the charge transport properties by using the rate-equation methods described above.

III. RESULTS AND DISCUSSIONS

In this section, we present the calculation results for the molecular junctions with the DW potentials. First, the charge transport properties of the molecular junction with electron-vibrational couplings described by displaced SDWPs are investigated and compared to that obtained with the HPs. The effect of breaking the symmetry of the two wells in the DW potential is then studied. Taking advantage of the unique vibrational transition properties of the ASDWPs, we also discuss the possibility of modulating the charge transport properties of such molecular junctions by applying external excitations that could lead to significant populations in the excited vibrational-energy levels.

A. Transport properties of molecular junctions with SDWPs

The charge transport properties of weakly coupled molecular junctions with electron-vibration coupling described by displaced HPs have been systematically studied previously [16,20,25,27,39]. Especially, it has been shown that increasing the strength of the electron-vibration couplings (which is dependent linearly on the displacement between the two potentials as $\lambda = \delta\sqrt{\omega/2\hbar}$) could lead to increased vibrational fine structures in the current-voltage (I-V) curves. Moreover, the FCB effect, where low-bias current was completely suppressed, can take place with strong electron-vibration couplings [16,39]. Both features can be found in

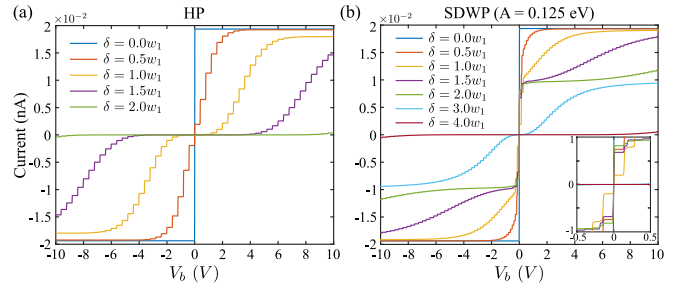


FIG. 3. I-V curves calculated at different displacement (δ) between the PESs of the initial and final states. (a) Displaced HPs, (b) displaced SDWPs. The insert in (b) is an enlarged view at low bias voltage.

Fig. 3(a), where we have calculated the I-V curves with increasing δ for the junction described by the displaced HPs. It can also be found that a clear FCB effect already started to take place at $\delta = w_1$.

Figure 3(b) demonstrates the I-V curves for the molecular junction described by displaced SDWPs. It can be found that although the low bias current also decreased with the increase of the displacement between the two PESs, the strong FCB effect as observed for the HP case was in fact completely lifted for displacements up to $2.0w_1$. A detailed analysis of the I-V curve in the range of -0.5 V to 0.5 V shows that at such small bias voltages the current first underwent a decrease with the increase of the displacement to the width of one well (nevertheless, it did not reach 0). Further increase of the displacement to $2.0w_1$ can actually recover the conductivity to be comparable with that obtained with $\delta = 0.5w_1$. For the cases with displacement around $2.0w_1$, it appears that the low bias current for the corresponding molecular junctions have reached a plateau with height around half of the saturated current. Detailed analysis of the I-V curve (see the SM for details) shows that the low-bias current first underwent a sharp increase to slightly smaller than half of the saturation current as obtained at $\delta = 0$. This rapid increase is caused by transitions involving the first two nearly degenerate vibrational levels. Due to the displacement of the PESs, only part of the wave functions in one of the two wells has significant contributions to the charge transport process via the overlaps with the wave functions of the other state, which gives the near half current. After the sharp increase, the transition to higher vibrational levels starts to contribute to the transport process through the small but nonzero vibrational overlaps, which causes the low-bias current to gradually increase. The current will eventually reach the saturated current at sufficiently high bias voltage that allows all of the vibrational transitions that could contribute to the transport process into the potential window. As can also be found in Fig. 3(b), further increasing the displacement to be larger than $2w_1$ again leads to the FCB effect, which is as expected because the remaining overlaps of the two SDWPs were further separated in a manner similar to that of the HPs. However, the calculation result indicates that the FCB effect might not be as prominent in molecular systems with SDWPs than those with HPs even when large nuclear rearrangement can happen upon electronic transitions. There are also other changes to the I-V characteristics of the SDWPs, especially the decreased energy spacing between adjacent current steps.

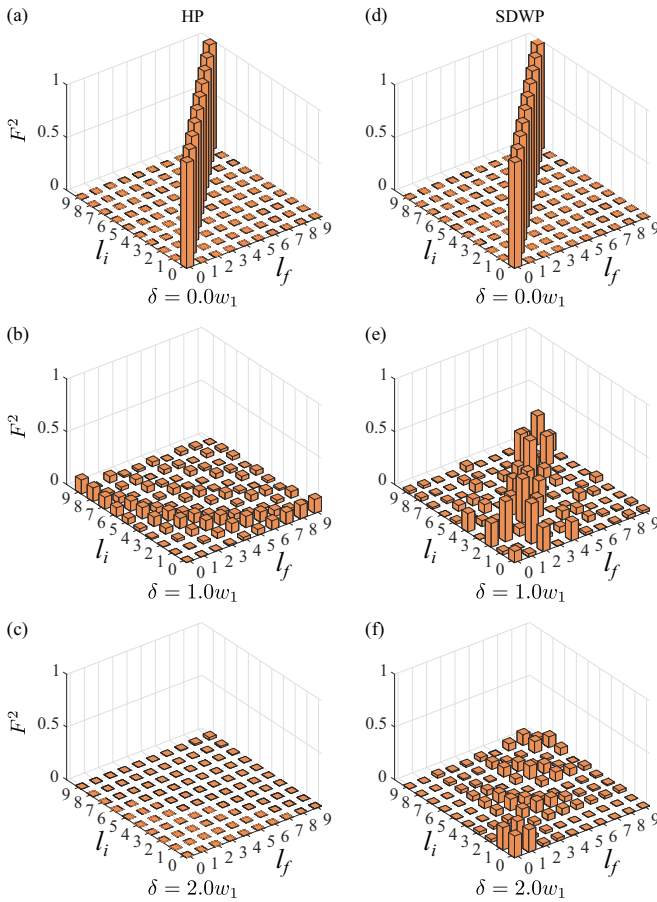


FIG. 4. The FC factors for the displaced HPs (a)–(c) and the displaced SDWPs (d)–(f). The displacement between the PESs has increased from 0 to $2.0w_1$ from top to bottom. l_i and l_f represent the vibrational levels of the initial and final states, respectively.

The different electron transport behaviors for the molecular junction with the SDWPs is clearly caused by the special properties of the vibrational structures of the PES. The reduced spacing between the current steps is a result of the more compacted energy levels of the SDWPs. The removal of the FCB effect at displacement up to $2.0w_1$ can be understood by the changes to the FC factors as shown in Fig. 4, where we have plotted out the two-dimensional FC matrix for the $l_i \rightarrow l_f$ vibrational transitions. l_i and l_f represent the vibrational levels of the initial and final states, respectively. The Z axis (F^2) is the square of FC factors. As can be found in Figs. 4(a) to 4(c), increasing the displacement for the displaced HP model could strongly suppress the FC factors for the low-lying vibrational transitions. At $\delta = 2.0w_1$, almost all of the transitions between the first ten vibrational levels in the two states are completely suppressed, which is responsible for the strong FCB effect shown in Fig. 3(a). In contrast, the vibrational transitions for the SDWPs with the same displacements are still active, as shown in Figs. 4(d) to 4(f). Especially, the FC factors for the 0-0 and 0-1 transitions still have relatively large values and remain open for the electron transport. Such different effects of increasing the displacement on the FC factors is attributed to the special distribution of the wave function of the ground vibrational state for the SDWPs. The even distribution

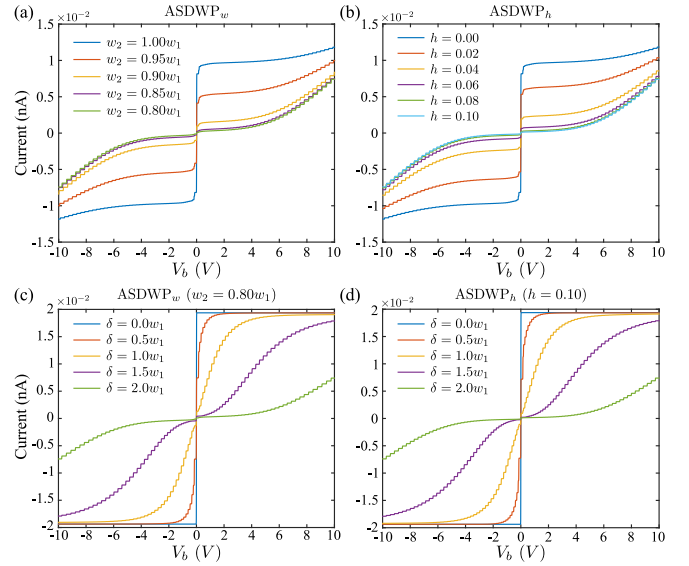


FIG. 5. I-V characteristics for the molecular junctions described by ASDWPs. (a) ASDWP_w with different decreasing widths (w_2) to one well. (b) ASDWP_h with different heights (h) to one well. δ has been set to $2w_1$ in (a) and (b). I-V curves obtained with increasing δ for ASDWP_w with $w_2 = 0.80w_1$ and ASDWP_h with $h=0.10$ a.u. are shown in (c) and (d), respectively.

ensures that even with relatively large displacement, the wave functions of the two electronic states still have significant overlaps. As a result, the FCB effect was suppressed at relatively large displacements in the displaced SDWP model. As we mentioned, further increasing the displacement of the SDWP model will lead to a HP-like decrease to the FC factors of the low-lying transitions and eventually will again cause the FCB effect as shown in Fig. 3(b).

B. Transport properties of molecular junctions with ASDWPs

As shown in Fig. 2, breaking the symmetry of the two wells in SDWPs could affect the vibrational structures of the resulting PESs. As a result, the removal of the FCB effect as observed for the molecular junction with SDWPs could also be affected. To examine such effect, we carried out calculations with molecular junctions described by ASDWPs with displacement large enough ($\delta = 2w_1$), which can cause significant FCBs in junctions with HPs [as shown in Fig. 3(a)]. Both two types of ASDWPs, ASDWP_w and ASDWP_h, were considered. The calculated I-V curves for these two types of ASDWPs with increasing asymmetries are shown in Figs. 5(a) and 5(b), respectively. It is clear that the current suppression starts to take place with the increase of the asymmetries of the PESs in both cases. For the strongly asymmetric cases of $w_2 = 0.80w_1$ and $h = 0.10$, the FCB effect was almost completely restored. We also investigated the influence of the displacement δ on the electron transport properties of the two types of ASDWPs. The calculation results are shown in Figs. 5(c) and 5(d), respectively. It can be found that the variation tendency of I-V curves of both ASDWP_w and ASDWP_h are similar to that of the junction with HPs shown in Fig. 3(a).

The similarities between the electron transport properties of the junctions with ASDWPs and HPs can be understood

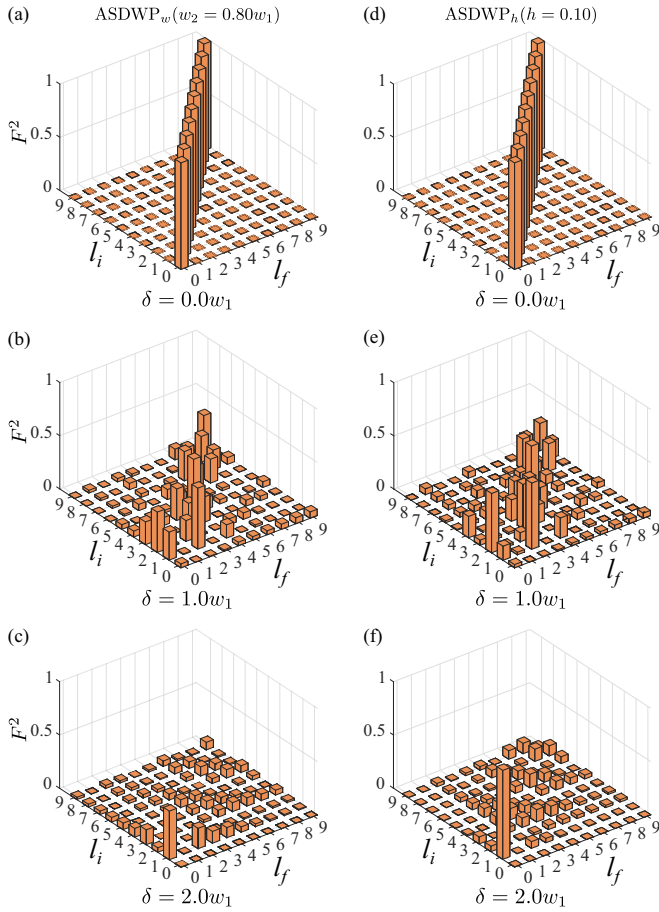


FIG. 6. The FC factors for the displaced $ASDWP_w$ with $w_2 = 0.80w_1$ (a)–(c), and $ASDWP_h$ with $h = 0.10$ a.u. (d)–(f).

from the vibrational wave functions of the ground level in the ASDWPs. As can be found in Figs. 2(c) and 2(d), breaking the symmetry of the two wells can break the degeneracy of the first two levels and, more importantly, make the ground vibrational level to be confined in one well instead of the even distribution in the two wells as found for the SDWPs. At low temperatures such as considered in the present paper, only the transition from the ground level to the final state will contribute significantly to the electron transport properties, which thus leads to the HP-like behaviors. Figure 6 shows the FC matrix of the two types of ASDWPs with increasing displacements. As can be clearly seen from Figs. 6(b), 6(c), 6(e), and 6(f), the FC factors for the $0_i \rightarrow l_f$ transitions undergo similar trends with those of the HPs [Figs. 4(b) and 4(c)] and were completely suppressed at larger displacements and, thus, lead to the FCB effect.

C. Influence of external excitation on the transport properties of molecular junctions with ASDWPs

An interesting feature that can be found from Fig. 6 is that the FC matrix is in fact quite different from that of the HPs, except the $0_i \rightarrow l_f$ transitions. Unlike in the case of the HPs where the FC factors for all the low-lying transitions are suppressed at large displacement, there are still many active transitions in the ASDWPs. Especially, a very strong

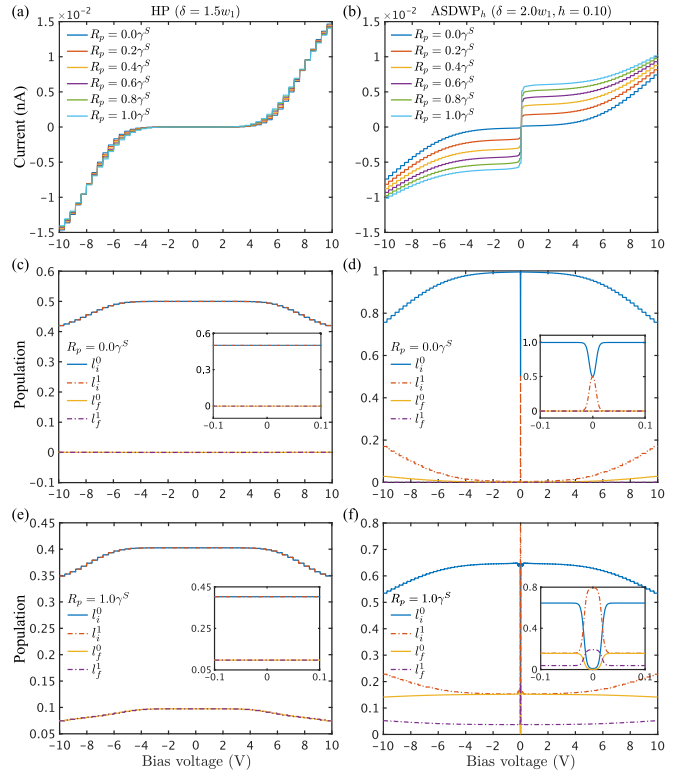


FIG. 7. I-V curves of (a) HP in the case of $\delta = 1.5w_1$ (b) $ASDWP_h$ in the case of $\delta = 2.0w_1, h = 0.10$.

$l_i \rightarrow 0_f$ transition can be found for the case of $\delta = 2.0w_1$. Normally, such transitions will not have large contributions to the current of the junctions due to the small populations of the excited vibrational energy levels (normally caused by the fast vibrational decay rates). However, the special transition properties indicate that the electron transport property of the corresponding molecular junction could be affected if such excited levels become involved in the transport processes. One possible way to achieve such a goal is to introduce external excitations such as infrared radiation. To investigate such an effect, we then performed model calculations by introducing a constant pumping rate from the ground vibrational level to the first excited vibrational level for molecular junctions described both by the HPs and ASDWPs in the interesting FCB regime.

The simulation results obtained by increasing the pumping rate from 0 to be equal to the bare tunneling rate of γ are illustrated in Figs. 7(a) and 7(b), respectively. Figures 7(c)–7(f) show the populations of the first two vibrational levels in each electronic states of the two types of PESs without [(c) and (d)] and with [(e) and (f)] external excitations. As can be found from Fig. 7(a), introducing such an excitation source only has a minor influence of the I-V curves of the molecular junction described by the HPs. Such behavior is as expected because the transitions from the first excited vibrational level are also strongly suppressed in the FCB regime. As a result, even if the excited level was populated, as shown in Figs. 7(c) and 7(e), the electric current will not change at low bias voltages. In contrast, increasing the pumping rate can lead to significant enhancement of the low-bias current and the removal of the

FCB effect. The increased current is a joint result of the increased population in the excited vibrational energy level [Figs. 7(d) and 7(f)] and the large transition probability of the $1_i \rightarrow 0_f$ transition. Such interesting results indicate that the electron transport properties of the molecular junctions with ASDWPs could be effectively modulated by suitable external excitations in the FCB regime.

IV. SUMMARY

In this paper, we studied the electron transport properties of a molecular junction described by DW potentials. It is found that the FCB effect caused by strong electron-vibration coupling in molecular junctions with HPs would be suppressed in junctions with SDWPs. Further calculations show that breaking the symmetry of the SDWP could restore the FCB effect. Such interesting transport phenomena are related to the unique vibrational structures of the DW potentials. In the case of SDWPs, the low-lying levels have even distributions in the two wells. Such a special structure ensures that the overlaps of the wave functions for the low-lying vibrational transitions in the SDWP cases do not undergo the monochromatic decrease

with the increase of the displacement between the shifted PESs as experienced by the HP models. As a consequence, the low-lying transitions still have significant contributions to the electronic transport process which led to the suppressed FCB effect. Such a feature is broken in ASDWPs due to the asymmetry of the two wells, which then leads to the restoration of the FCB effect. Taking advantage of the unique vibration transition properties of the ASDWPs, we showed that the electron transport properties of molecular junctions with such potentials can be effectively modulated in the FCB regime by introducing external excitations. The results obtained in the present paper not only supplied a detailed analysis on the special transport properties of molecular junctions with DWPs, but also offered a viable way to control the transport properties of molecular junctions, which could be helpful for the design of functional molecular devices.

ACKNOWLEDGMENTS

This work was supported by the National Natural Science Foundation of China (Grant No. 21973081) and the 100 Talents Project of Hebei Province (Grant No. E2016100003).

-
- [1] A. Aviram and M. A. Ratner, *Chem. Phys. Lett.* **29**, 277 (1974).
 [2] A. Nitzan, *Annu. Rev. Phys. Chem.* **52**, 681 (2001).
 [3] S. V. Aradhya and L. Venkataraman, *Nat. Nanotechnol.* **8**, 399 (2013).
 [4] M. L. Perrin, E. Burzurí, and H. S. van der Zant, *Chem. Soc. Rev.* **44**, 902 (2015).
 [5] D. Xiang, X. Wang, C. Jia, T. Lee, and X. Guo, *Chem. Rev.* **116**, 4318 (2016).
 [6] N. Xin, J. Guan, C. Zhou, X. Chen, C. Gu, Y. Li, M. A. Ratner, A. Nitzan, J. F. Stoddart, and X. Guo, *Nat. Rev. Phys.* **1**, 211 (2019).
 [7] P. Gehring, J. M. Thijssen, and H. S. van der Zant, *Nat. Rev. Phys.* **1**, 381 (2019).
 [8] F. Evers, R. Korytár, S. Tewari, and J. M. van Ruitenbeek, *Rev. Modern Phys.* **92**, 035001 (2020).
 [9] R. Gaudenzi, M. Misiorny, E. Burzurí, M. R. Wegewijs, and H. S. van der Zant, *J. Chem. Phys.* **146**, 092330 (2017).
 [10] L. Yuan, N. Nerngchamnong, L. Cao, H. Hamoudi, E. Del Barco, M. Roemer, R. K. Sriramula, D. Thompson, and C. A. Nijhuis, *Nat. Commun.* **6**, 6324 (2015).
 [11] C. Jia, A. Migliore, N. Xin, S. Huang, J. Wang, Q. Yang, S. Wang, H. Chen, D. Wang, B. Feng *et al.*, *Science* **352**, 1443 (2016).
 [12] X. Chen, M. Roemer, L. Yuan, W. Du, D. Thompson, E. Del Barco, and C. A. Nijhuis, *Nat. Nanotechnol.* **12**, 797 (2017).
 [13] X. Yin, Y. Zang, L. Zhu, J. Z. Low, Z.-F. Liu, J. Cui, J. B. Neaton, L. Venkataraman, and L. M. Campos, *Sci. Adv.* **3**, ea02615 (2017).
 [14] M. Galperin, M. A. Ratner, and A. Nitzan, *J. Phys.: Condens. Matter* **19**, 103201 (2007).
 [15] J. M. Thijssen and H. S. Van der Zant, *Phys. Status Solidi B* **245**, 1455 (2008).
 [16] J. Koch and F. von Oppen, *Phys. Rev. Lett.* **94**, 206804 (2005).
 [17] J. S. Seldenthuis, H. S. Van Der Zant, M. A. Ratner, and J. M. Thijssen, *ACS Nano* **2**, 1445 (2008).
 [18] G. Tian, D. Sun, Y. Zhang, and X. Yu, *Angew. Chem. Int. Ed.* **58**, 5951 (2019).
 [19] R. Leturcq, C. Stampfer, K. Inderbitzin, L. Durrer, C. Hierold, E. Mariani, M. G. Schultz, F. Von Oppen, and K. Ensslin, *Nat. Phys.* **5**, 327 (2009).
 [20] G. Tian and Y. Luo, *J. Phys. Chem. C* **118**, 14853 (2014).
 [21] E. Burzurí, Y. Yamamoto, M. Warnock, X. Zhong, K. Park, A. Cornia, and H. S. van der Zant, *Nano Lett.* **14**, 3191 (2014).
 [22] C. S. Lau, H. Sadeghi, G. Rogers, S. Sangtarash, P. Dallas, K. Porfyrakis, J. Warner, C. J. Lambert, G. A. D. Briggs, and J. A. Mol, *Nano Lett.* **16**, 170 (2016).
 [23] J. Koch and F. von Oppen, *Phys. Rev. B* **72**, 113308 (2005).
 [24] F. Elste and F. von Oppen, *New J. Phys.* **10**, 065021 (2008).
 [25] G. Tian, S. Duan, G.-P. Zhang, W. Hu, and Y. Luo, *Phys. Chem. Chem. Phys.* **17**, 23007 (2015).
 [26] H. M. Friedman, B. K. Agarwalla, and D. Segal, *J. Chem. Phys.* **146**, 092303 (2017).
 [27] D. Sun, L. Li, X. Yu, and G. Tian, *Phys. Rev. B* **99**, 125423 (2019).
 [28] H. A. Jahn and E. Teller, *Proc. R. Soc. London A* **161**, 220 (1937).
 [29] E. Bonet, M. M. Deshmukh, and D. C. Ralph, *Phys. Rev. B* **65**, 045317 (2002).
 [30] K. D. McCarthy, N. Prokof'ev, and M. T. Tuominen, *Phys. Rev. B* **67**, 245415 (2003).
 [31] G. Tian, J.-C. Liu, and Y. Luo, *Phys. Rev. Lett.* **106**, 177401 (2011).
 [32] V. Jelic and F. Marsiglio, *European J. Phys.* **33**, 1651 (2012).
 [33] M. Baradaran and H. Panahi, *Adv. High Energy Phys.* **2017**, 2181532 (2017).
 [34] See Supplemental Material at <http://link.aps.org/supplemental/10.1103/PhysRevB.104.245411> for the influence of barrier

- height on the transport properties of molecular junctions described by displaced SDWPs and detailed analysis of the low-bias current for the junction with SDWPs.
- [35] M. G. Schultz and F. von Oppen, *Phys. Rev. B* **80**, 033302 (2009).
- [36] M. Leijnse and M. R. Wegewijs, *Phys. Rev. B* **78**, 235424 (2008).
- [37] G. Theocharis, P. G. Kevrekidis, D. J. Frantzeskakis, and P. Schmelcher, *Phys. Rev. E* **74**, 056608 (2006).
- [38] N. Mukherjee and A. K. Roy, *Ann. Phys.* **528**, 412 (2016).
- [39] J. Koch, F. von Oppen, and A. V. Andreev, *Phys. Rev. B* **74**, 205438 (2006).